Atmospheric
Chemistry
and Physics
Discussions

**Biomass
burning-tropopause
mixing**

J. Brioude et al.

Title Page

Abstract	Introduction
Conclusions	References
Tables	Figures

◄◄   ►►

◄   ►

Back   Close

Full Screen / Esc

Printer-friendly Version

Interactive Discussion

EGU

Mixing between a stratospheric intrusion and a biomass burning plume

**J. Brioude[1], O. R. Cooper[1,2], M. Trainer[1], T. B. Ryerson[1], J. S. Holloway[1,2],
T. Baynard[1,2], J. Peischl[1,2], C. Warneke[1,2], J. A. Neuman[1,2], J. De Gouw[1,2],
A. Stohl[3], S. Eckhardt[3], G. J. Frost[1,2], S. A. McKeen[1,2], E.-Y. Hsie[1,2],
F. C. Fehsenfeld[1,2], and P. Nédélec[4]**

[1]Chemical Sciences Division, Earth Science Reasearch Laboratory, NOAA, Boulder,
Colorado, USA
[2]Cooperative Institute for Research in Environmental Sciences, University of Colorado,
Boulder, Colorado, USA
[3]Norwegian Institute for Air Research, Kjeller, Norway
[4]Laboratoire d'Aérologie, UMR 5560, Observatoire Midi-Pyrénées, Toulouse, France

Correspondence to: J. Brioude (jerome.brioude@noaa.gov)

Biomass burning-tropopause mixing

J. Brioude et al.

Title Page

Abstract	Introduction
Conclusions	References
Tables	Figures

◄◄	►►
◄	►
Back	Close

Full Screen / Esc

Printer-friendly Version

Interactive Discussion

EGU

Abstract

Ozone, carbon monoxide, aerosol extinction coefficient, acetonitrile, nitric acid and relative humidity measured from the NOAA P3 aircraft during the TexAQS/GoMACCS 2006 experiment, indicate mixing between a biomass burning plume and a stratospheric intrusion in the free troposphere above eastern Texas. Lagrangian-based transport analysis and satellite imagery are used to investigate the transport mechanisms that bring together the tropopause fold and the biomass burning plume originating in southern California, which may affect the chemical budget of tropospheric trace gases.

1 Introduction

Since the pioneering work of Danielsen (1968), tropopause folds have been a focus of atmospheric research because they are the main source of stratospheric ozone flux into the troposphere. Recently, much attention has been paid to the decay of tropopause folds in the troposphere because they affect the *OH* radical concentration and the chemical budget of different trace gases in the troposphere (Esler et al., 2001). Previous studies have shown that tropopause folds can disperse into decaying warm conveyor belts (Cooper et al., 2004), and they can also be interleaved with anthropogenic pollution (Cho et al., 2001; Parrish et al., 2000). Irreversible Stratosphere-Troposphere Exchange (STE) occurs between these layers at small scale resulting in a layer with elevated ozone and reduced CO relative to adjacent unimpacted tropospheric air.

In this case study, we present new insight on STE by reporting on the mixing between a tropopause fold and a biomass burning (BB) plume in the free troposphere. BB is known to be one of the main sources of aerosols, carbon monoxide (CO), volatile organic compounds and nitrogen oxides (NOx) in the troposphere (Andreae and Merlet, 2001). It can also affect ozone concentrations at the continental scale (Wotawa

and Trainer, 2000; Mckeen et al., 2002). However, to date, mixing between a BB plume and a tropopause fold has not been documented. The event occurred during the Texas Air Quality Study/Gulf of Mexico Atmospheric Composition and Climate Study (TexAQS/GoMACCS). The experiment was conducted during August-October 2006 across eastern Texas and the northwestern Gulf of Mexico. A major focus of Tex-AQS/GoMACCS is the influence of anthropogenic trace gases and aerosol emissions on the air quality and radiative balance of east Texas and the Gulf of Mexico. Here we describe analyses of several in-situ measurements using numerical simulations with a Lagrangian particle dispersion model and satellite imagery.

2 Method

2.1 In-situ measurements

CO on the NOAA WP-3D research aircraft was measured once per second using using vacuum ultraviolet resonance fluorescence (Holloway et al., 2000) with an uncertainty of ±5%. Ozone was measured with an uncertainty of ±(0.1 ppbv + 3%).

The aerosol extinction coefficient (σ_{ep}, 532 nm, 10% RH) was measured using a cavity ring-down technique and dried to RH≤10 with an uncertainty of ±5% (Baynard et al., 2006).

Acetonitrile was measured with a PTR-MS instrument for 1 s every 17 s (de Gouw and Warneke, 2007) with an uncertainty of ±15%.

Gas phase nitric acid (HNO_3) was measured once per second using a chemical ionization mass spectrometer (Neuman et al., 2002) with a precision of ±20 pptv and an accuracy of ±(15% + 100 pptv).

2.2 Model description

To identify the origin of the polluted plume and simulate air pollution transport over North America, we use the FLEXPART Lagrangian particle dispersion model (version

6.2) (Stohl et al., 2005 and references therein). We conducted forward simulations of long-range and mesoscale transport of anthropogenic pollution tracers from North America and emissions from BB to assess their impact on observed CO concentrations over Texas and the Gulf of Mexico. FLEXPART was driven by model-level data from the European Centre for Medium-Range Weather Forecasts (ECMWF), with a temporal resolution of 3 h (analyses at 00:00, 06:00, 12:00, 18:00 UTC ; 3-h forecasts at 03:00, 09:00, 15:00, 21:00 UTC), and 91 vertical levels. Horizontal resolution was $1°×1°$ globally with nested wind fields at $0.36°×0.36°$ resolution ($108°$ W–$27°$ W, $9°$ N–$54°$ N). Anthropogenic CO emissions from Canada and Mexico were taken from the EDGAR 2000 inventory at $1°×1°$ resolution. Tracer particles were injected between 0 and 150 m above ground level, representing the mean injection height of point sources and distributed area surface emissions. CO emissions from the United States were based on the EPA 1999 National Emission Inventory at 4 km×4 km resolution (Frost et al., 2006). Injection height of point sources in the model is specified in the inventory, while the mean injection height of area sources was between 0 and 20 m. BB CO emissions were calculated using the algorithm of Stohl et al. (2007), which uses fire detection data, information on landuse and applies emission factors from Andreae and Merlet (2001). We used an injection height between 0 and 5 km, and assessed the area burned with the National Interagency Coordination Center Incident Management Report of forest fires. The passive BB CO tracer was allowed to advect for either 5 or 15 days, after which it was removed from the simulation. A stratospheric ozone tracer was initialized within the model domain and continually released at the model boundaries ($130°$ W–$55°$ W, $10°$ N–$61°$ N), and allowed to advect with ECMWF winds within the domain (Stohl et al., 2000; Cooper et al., 2005). A linear relationship between ozone and potential vorticity of 50 ppbv/pvu was used for the month of September (Stohl et al., 2000). The stratospheric ozone is treated as a passive tracer, and its distribution in the troposphere is only due to transport from the stratosphere. Concentration fields were output every hour as 1-h averages at $0.6°×0.6°$ grid spacing above the USA and Mexico, and $0.15°×0.15°$ grid spacing above Texas and the Gulf of Mexico. The FLEX-

Title Page

Abstract | Introduction

Conclusions | References

Tables | Figures

◄ | ►|

◄ | ►

Back | Close

Full Screen / Esc

Printer-friendly Version

Interactive Discussion

EGU

PART tracers are only 15 days old and must be considered as mixing ratios above background. In addition, backward simulations started along the aircraft flight track were used to retrieve the distribution of the different source regions of the pollutants.

3 Analysis

⁵ Figure 1 presents time series of (top) ozone, CO, σ_{ep}, HNO$_3$ (pptv), acetonitrile (CH$_3$CN, pptv/2) and (bottom) measurements of altitude and relative humidity, over Texas from the NOAA P3 aircraft flight on 25 September 2006.

σ_{ep} and acetonitrile (de Gouw et al., 2003; Warneke et al., 2006) can be used as biomass burning tracers. Positive correlations between CO, σ_{ep} and acetonitrile indi-¹⁰ cate the biomass burning origin of CO enhancements. HNO$_3$ can be used as a strato-spheric tracer. Positive correlations between HNO$_3$ and ozone indicate a stratospheric origin of ozone enhancements.

At 4km altitude, a CO peak (up to 220 ppbv) is followed by an ozone peak (up to 80 ppbv) around 16:10 UTC. The only significant σ_{ep} and acetonitrile enhancement ¹⁵ occurs during the time period of the main two CO peaks. The enhancements of CO, σ_{ep} and acetonitrile and their enhancement ratios to CO$_2$ (not shown) suggest a biomass burning origin rather than anthropogenic pollution.

From 16h05 to 16h15, the enhancement of ozone (from 30 to 80 ppbv) is positively correlated with the nitric acid (from 30 to 150 pptv) and negatively correlated with rel-²⁰ ative humidity. The HNO$_3$ to ozone slope is HNO$_3$=0.0022*O$_3$–0.055, and is consis-tent with previous measurements obtained in the lower stratosphere where the typical HNO$_3$ mixing ratio at the tropopause is 300pptv in September (Neuman et al., 2001).

Figure 2 compares the observed ozone and CO measurements from Fig. 1 (colored dots) to the ozone and CO distributions in the free troposphere (top) and the entire tro-²⁵ posphere/lowermost stratosphere (bottom) retrieved from MOZAIC (Measurements of Ozone, Water Vapour, Carbon Monoxide and Nitrogen Oxides by Airbus in service air-craft, Thouret et al., 1998; Nedelec et al., 2003) profiles (grey background) over Hous-

ton, Dallas and Atlanta, in September 2003 and 2004. Most of the MOZAIC ozone and CO mixing ratios in the free troposphere are between 40 and 60 ppbv of ozone and 70 to 100 ppbv of CO. Comparing Fig. 2(top) and (bottom), the vertical branch of Fig. 2(bottom) is related to upper tropospheric measurements while the horizontal branch is related to lower tropospheric measurements. Two processes are visible in the P3 data in this figure. The first one is exemplified by the positive correlation between ozone and CO. It may be related to photochemical production of ozone in a pollution plume (with up to 200 ppbv of CO, 50 ppbv of ozone).The second process is demonstrated by a negative correlation between ozone and CO with two different negative slopes. This process may be due to STE (e.g. Hoor et al., 2002), since negative ozone/CO slopes seen in MOZAIC data are related to the mean vertical branch of the upper troposphere.

Figure 1(bottom) shows the time series of the modeled BB and anthropogenic CO tracers and the stratospheric ozone tracer, from the nested domain output, linearly interpolated along the aircraft flight track. At about 16:10 UTC, a well-defined BB CO tracer peak lies at the same position as the P3 CO and σ_{ep} peaks, while a small anthropogenic tracer contribution is modeled at this time. The BB CO tracer peak is underestimated (35 ppbv) compared with the P3 CO peak (up to 120 ppbv above the CO background). However, the width of the P3 CO peak is about 6 km (1 min with an aircraft ground speed of 100 ms^{-1}) which is quite small compared to the simulation output scale (0.15°×0.15°). The integral of the measured CO enhancement relative to the background is 14 864 ppbv s, while the integrated modeled BB CO peak is 14 115 ppbv s, or about 95% of the integrated measurement. Thus, the model suggests that the sampled CO peak is mainly due to a BB plume.

The modeled anthropogenic CO tracer is correlated with measured CO except at the time of the two main CO peaks. At 16:00 UTC, the P3 background CO is about 65 ppbv while the modeled anthropogenic CO tracer is close to zero. Backward trajectories give a Pacific Ocean origin for this time period (not shown). At 16:15 UTC the measured background CO is about 95 ppbv and the modeled anthropogenic CO

EGU

tracer is 20 ppbv. This airmass comes from western Texas, New Mexico and Arizona (not shown). Therefore the increase in measured background CO (30 ppbv) is due to influence from anthropogenic pollution.

Figure 2 is colored by the modeled stratospheric ozone tracer (bottom) and by the BB CO tracer (top). The 5-day BB tracer shows that the positive correlation between ozone and CO (from 30 ppbv of ozone and 100 ppbv of CO to 50 ppbv of ozone and 180 ppbv of CO) is related to mixing between relatively clean background air and the biomass burning plume. The stratospheric ozone tracer indicates that an air mass with a significant stratospheric component (100 ppbv of CO and 80 ppbv of ozone) mixed with both a relatively clean tropospheric airmass (115 ppbv of CO and 55 ppbv of ozone) and the BB plume (200 ppbv of CO and 50 ppbv of ozone). Applying a 15-day BB CO tracer only increases the BB CO peak value by 2 ppbv. Therefore the BB plume appears to be primarily less than 5 days old.

The anticorrelations between the BB CO and stratospheric ozone tracers, P3 ozone and CO, and P3 relative humidity and CO, reinforce the hypothesis of mixing between a stratospheric intrusion and a biomass burning plume.

Figure 3 (top) presents the visible channel of the GOES-East satellite at 13:15 UTC, 25 September, 3 h before the aircraft sampled the BB plume. A narrow plume is visible north of the aircraft position at 16:10 UTC (red cross), and extends from eastern Texas to western New Mexico. This narrow plume is only visible at sunrise when the sun is low in the sky and the underlying surface is not bright.

FLEXPART backward calculations were used to locate the source region of the BB CO that contributed to the two P3 CO peaks. Figure 4 presents the percentage of surface contribution to the BB CO mixing ratios, scaled according to the maximum surface contribution encountered in the domain output (red pixel). It shows that the main source is located north of Los Angeles.

On 21 September 20:30 UTC (Fig. 3 bottom), the visible channel of the MODIS satellite instrument shows a large forest fire located in the Los Padres National Forest north of Los Angeles at the same location as the BB contribution simulated by FLEX-

PART. The NASA Earth Observatory (http://earthobservatory.nasa.gov/Newsroom/ NewImages/images.php3?img_id=17408) reports that this fire began on September 4 and burned with varying intensity until the end of September.

A supplemental animation (http://www.atmos-chem-phys-discuss.net/7/8017/2007/ acpd-7-8017-2007-supplement.zip) shows the transport of the modeled BB plume from this forest fire (blue) and the transport of stratospheric intrusions (green), for the period 12:00 UTC 21 September to 18:00 UTC 25 September. Red areas represent mixing regions where the BB plume and stratospheric intrusion are colocated. From 12:00 UTC 21 September to 12:00 UTC September 22 the BB plumes produced near Los Angeles remained in the southwestern United States. During this time a large upper level low became established above the central United States with a strong cold front draped across the south-central USA. This system produced westerly flow in the lower and mid-troposphere across the western USA which allowed a portion of the BB plume to reach the eastern USA by 12:00 UTC 23 September. The influence of the upper level low persisted and other portions of the BB plume advected eastward from southern California on 24 September until they reached east Texas on September 25. Meanwhile a large and deep stratospheric intrusion produced by the upper level low penetrated into the lower troposphere and advected eastward with the same flow pattern along the poleward edge of the BB plume. By 03:00 UTC 24 September portions of the stratospheric intrusion began to disperse into the BB plume above the southwestern USA (red regions in the movie). The plumes continued to mingle as they advected eastward. At 15:00 UTC 25 September, the southern part of the comingled plumes was located above east Texas where the NOAA P3 aircraft sampled it at 16:10 UTC.

Figure 5 (bottom) presents a horizontal cross section of the FLEXPART stratospheric ozone tracer at 4 km altitude and the mean BB CO tracer between 3 and 5 km altitude. The BB plume lies next to the tropopause fold from Texas to the Great Lakes region. The narrow BB plume seen in the GOES image (Fig. 3, top) is well simulated by FLEX-PART (Fig. 5, bottom). Figure 5 (top) presents a meridional vertical cross section at the longitude of the aircraft position at 16:10 UTC (black circle in Fig. 5, bottom). A

potential mixing region (red pixels) is identified between 3 and 5 km, using a threshold of 10 ppbv for the BB CO tracer and 15 ppbv for the stratospheric ozone tracer, in the vicinity of the NOAA P3 aircraft (black circle).

4 Discussion

This Lagrangian-based study confirms that mixing does occur between biomass burning plumes and stratospheric intrusions in the free troposphere. To assess the frequency of these events, we performed a statistical analysis using the FLEXPART forward simulations from 1 August to 1 October 2006 above the Texas and Gulf of Mexico region. We used the same FLEXPART simulations for stratospheric tracers and biomass burning, assuming an area burned of 180 ha per fire detection (Stohl et al., 2007). When a stratospheric intrusion (ozone tracer$\geq$30ppbv) was present in this region, some portion of it was co-located with biomass burning plumes (BB CO tracer$\geq$ 10 ppbv) 63% of the time at the surface (2 stratospheric intrusions events), 74% between 100 m and 4 km of altitude (6 events), 28% between 4 and 8 km (9 events) and 11% above 8 km. The percentage decreases with altitude because the biomass burning plumes are less frequent in the free and upper troposphere. These results imply that mixing between stratospheric intrusions and biomass burning plumes can influence tropospheric chemistry and may have implications for surface air quality.

References

Andreae, M. O. and Merlet, P.: Emission of trace gases and aerosols from biomass burning, Global Biogeochem. Cycles, 15, 955–966, 2001.

Baynard, T., Garland, R. M., Ravishankara, A. R., Tolbert, M. A., and Lovejoy, E. R.: Key factors influencing the relative humidity dependence of aerosol light scattering, Geophys. Res. Lett., 33, L06813, doi:10.1029/2005GL024898, 2006.

Cho, J. Y. N., Newell, R. E., Browell, E. V., Grant, W. B., Butler, C. F., and Fenn, M. A.: Observation of pollution plume capping by a tropopause fold, Geophys. Res. Lett., 28, 3243–3246, 2001.

Cooper, O. R., Forster, C., Parrish, D., Dunlea, E., Hubler, G., Fehsenfeld, F., Holloway, J., Oltmans, S., Johnson, B., Wimmers, A., and Horowitz, L.: On the life-cycle of a stratospheric intrusion and its dispersion into polluted warm conveyor belts, J. Geophys. Res., 109, D23S09, doi:10.1029/2003JD004006, 2004.

Cooper, O. R., Stohl, A., Hubler, G., Hsie, E. Y., Parrish, D. D., Tuck, A. F., Kiladis, G. N., Oltmans, S. J., Johnson, B. J., Shapiro, M., Moody, J. L., and Lefohn, A. S.: Direct transport of midlatitude stratospheric ozone into the lower troposphere and marine boundary layer of the tropical Pacific Ocean, J. Geophys. Res., 110, D23310, doi:10.1029/2005JD005783, 2005.

Danielsen, E. F.: Stratospheric-tropospheric exchanges based upon radioactivity, ozone and potential vorticity, J. Atmos. Sci., 25, 502–518, 1968

de Gouw, J. A., Warneke, C., Parrish, D. D., Holloway, J. S., Trainer, M., and Fehsenfeld, F. C.: Emission sources and ocean uptake of acetonitrile (CH3CN) in the atmosphere, J. Geophys. Res., 108(D11), 4329, doi:10.1029/2002JD002897, 2003.

de Gouw, J. and Warneke, C.: Measurements of volatile organic compounds in the earths atmosphere using proton-transfer-reaction mass spectrometry, Mass Spectrom. Rev., 26(2), 223–257, 2007.

Esler J. G., Tan, D. G. H., Haynes, P. H., Evans, M. J., Law, K. S., Plantevin, P. H., and Pyle, J. A.: Stratosphere-troposphere exchange: Chemical sensitivity to mixing, J. Geophys. Res., 106(D5), 4717–4731, doi:10.1029/2000JD900405, 2001.

Frost, G. J., McKeen, S. A., Trainer, M., et al.: Effects of changing power plant NOx emissions on ozone in the eastern United States: Proof of concept, J. Geophys. Res., 111, D12306, doi:10.1029/2005JD006354, 2006.

Biomass burning-tropopause mixing

J. Brioude et al.

Title Page

Abstract	Introduction
Conclusions	References
Tables	Figures

◄◄   ►►

◄   ►

Back   Close

Full Screen / Esc

Printer-friendly Version

Interactive Discussion

EGU

Holloway, J. S., Jakoubek, R. O., Parrish, D. D., Gerbig, C., Volz-Thomas, A., Schmitgen, S., Fried, A., Wert, B., B.,, and Drummond, J. R.: Airborne intercomparison of vacuum ultraviolet fluorescence and tunable diode laser absorption measurements of tropospheric carbon monoxide, J. Geophys. Res., 105(D19), 24 251–24 262, 2000.

Honrath, R. E., Owen, R. C., Val Martin, M., Reid, J. S., Lapina, K., Fialho, P., Dziobak, M. P., Kleissl, J., and Westphal, D. L.: Regional and hemispheric impacts of anthropogenic and biomass burning emissions on summertime CO and O3 in the North Atlantic lower free troposphere, J. Geophys. Res., 109, D24310, doi:10.1029/2004JD005147, 2004.

Hoor, P., Fischer, H., Lange, L., Lelieveld, J., and Brunner, D.: Seasonal variations of a mixing layer in the lowermost stratosphere as identified by the CO-O3 correlation from in situ measurements, J. Geophys. Res., 107(D5), 4044, doi:10.1029/2000JD000289, 2002.

McKeen, S. A., Wotawa, G., Parrish, D. D., Holloway, J. S., Buhr, M. P., Hubler, G., Fehsenfeld, F. C., and Meagher, J. F.: Ozone production from Canadian wildfires during June and July of 1995, J. Geophys. Res., 107(D14), 4192, doi:10.1029/2001JD000697, 2002.

Nedelec, P., Cammas, J. -P., Thouret, V., Athier, G., Cousin, J. -M., Legrand, C., Abonnel, C., Lecoeur, F., Cayez, G., and Marizy, C.: An improved infrared carbon monoxide analyser for routine measurements aboard commercial Airbus aircraft: technical validation and first scientific results of the MOZAIC III programme, Atmos. Chem. Phys., 3, 1551–1564, 2003, http://www.atmos-chem-phys.net/3/1551/2003/.

Neuman, J. A., McKeen, S. A., Trainer, M., et al.: Fast-response airborne in situ measurements of HNO3 during the Texas Air Quality Study, J. Geophys. Res., 107(D20), 4436, doi:10.1029/2001JD001437, 2002.

Parrish, D. D., Holloway, J. S., Jakoubek, R., Trainer, M., Ryerson, T. B., Hubler, G., Fehsenfeld, F. C., Moody, J. L., and Cooper, O. R.: Mixing of anthropogenic pollution with stratospheric ozone: A case study from the North Atlantic wintertime troposphere, J. Geophys. Res., 105, 24 363–24 374, 2000.

Reid, H. J. and Vaughan, G.: Convective mixing in a tropopause fold, Q. J. R. Meteorol. Soc.,130, 1195-1221, 2004.

Stohl, A., Spichtinger-Rakowsky, N., Bonasoni, P., Feldmann, H., Memmesheimer, M., Scheel, H. E., Trickl, T., Hubener, S. H., Ringer, W., and Mandl, M.: The influence of stratospheric intrusions on alpine ozone concentrations, Atmos. Environ., 34, 1323–1354, 2000.

Stohl, A., Forster, C., Frank, A., Seibert, P., and Wotawa, G.: Technical note: The Lagrangian particle dispersion model FLEXPART version 6.2., Atmos. Chem. Phys., 5, 2461–2474,

2005,
http://www.atmos-chem-phys.net/5/2461/2005/.

Stohl, A., Berg, T., Burkhart, J. E., et al.: Arctic smoke-record high air pollution levels in the European Arctic due to agricultural fires in Eastern Europe, Atmos. Chem. Phys., 7, 511–534, 2007,
http://www.atmos-chem-phys.net/7/511/2007/.

Thouret, V., Marenco, A., Nedelec, P., and Grouhel, C.: Ozone climatologies at 9–12 km altitude as seen by the MOZAIC airborne program between September 1994 and August 1996, J. Geophys. Res., 103, 25 653–25 679, 1998.

Warneke, C., de Gouw J. A., Stohl, A., et al.: Biomass burning and anthropogenic sources of CO over New England in the summer 2004, J. Geophys. Res., 111, D23S15, doi:10.1029/2005JD006878, 2006.

Wotawa, G. and Trainer, M.: The influence of Canadian forest fires on pollutant concentrations in the United States, Science, 288, 324–328, 2000.

Title Page

Abstract | Introduction

Conclusions | References

Tables | Figures

◄◄ | ►►

◄ | ►

Back | Close

Full Screen / Esc

Printer-friendly Version

Interactive Discussion

EGU

Biomass burning-tropopause mixing

J. Brioude et al.
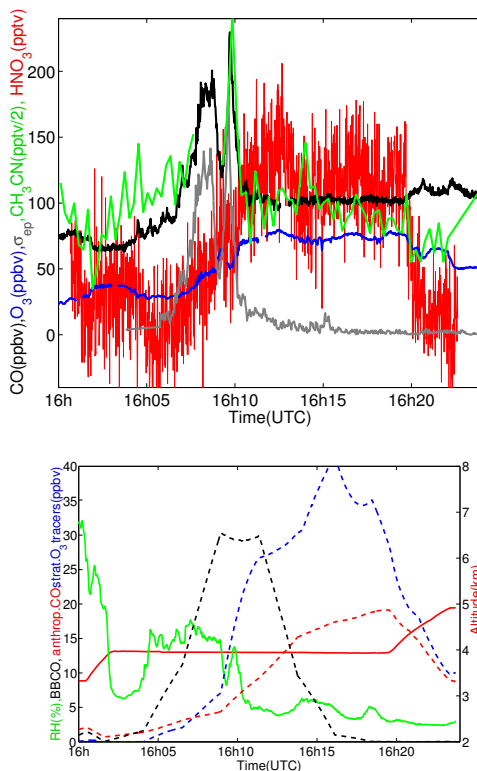
Fig. 1. Top: NOAA P3 time series of CO (black line, ppbv), ozone (blue line, ppbv), σ_{ep} (gray line, Mm^{-1}), acetonitrile (green line, pptv/2) and nitric acid (red line, pptv) on September 25 between 16:00 and 16:25 UTC.
Bottom NOAA P3 time series of altitude (red solid line, km) and relative humidity (green solid line, %, right vertical axis). Also shown are the FLEXPART biomass burning CO tracer (black dashed line, ppbv), anthropogenic CO tracer (red dashed line, ppbv) and stratospheric ozone tracer (blue dashed line, ppbv).
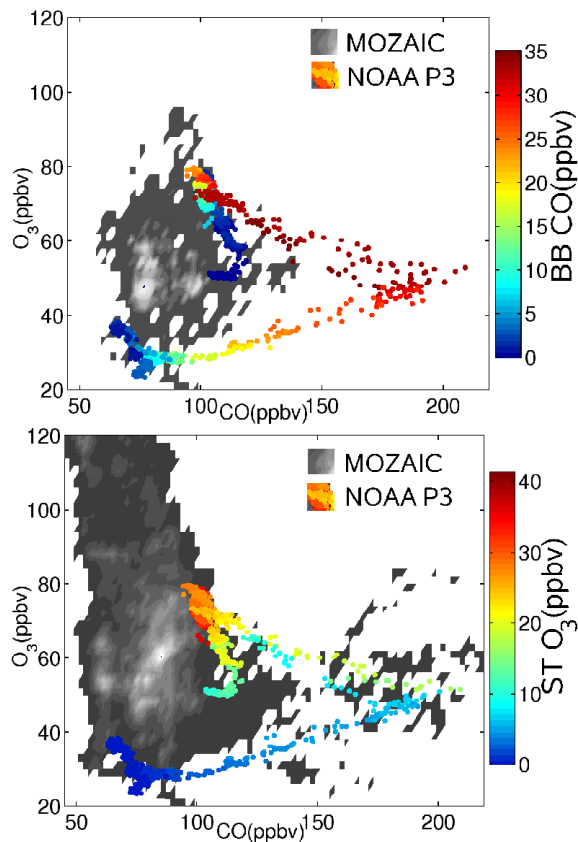
Fig. 2. NOAA P3 ozone and CO mixing ratios on 25 September, 16:00–16:25 UTC, colored by (top) the modeled biomass burning CO tracer and (bottom) by the stratospheric ozone tracer. The grey background represents the distribution of MOZAIC ozone and CO measurements in (top) the free troposphere (defined by 300 hPa≤pressure≤800 hPa) and (bottom) the entire troposphere/lowermost stratosphere (pressure≥300 hPa). Lighter (darker) shading indicates a greater (lesser) number of measurements.

Title Page

Abstract | Introduction

Conclusions | References

Tables | Figures

◄◄ | ►►

◄ | ►

Back | Close

Full Screen / Esc

Printer-friendly Version

Interactive Discussion

EGU
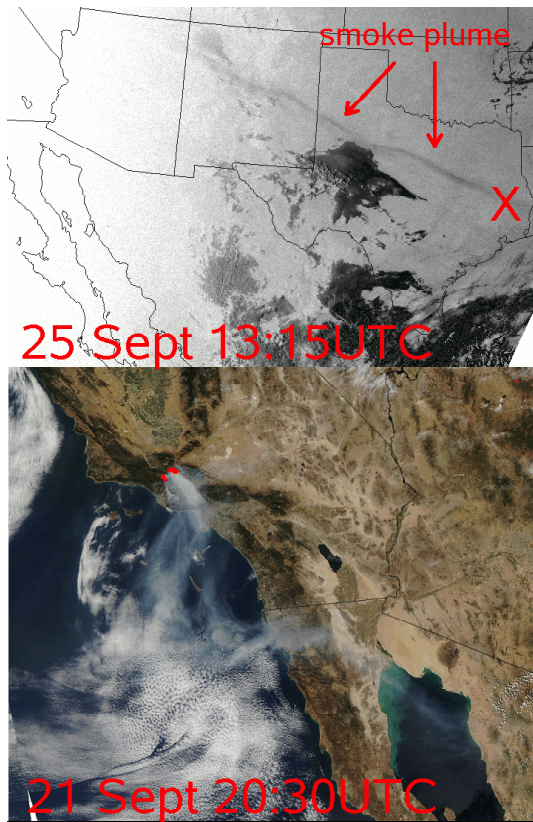
Fig. 3. Top: Visible channel of the GOES East imager, 13:15 UTC 25 September. Dark areas represent clouds or aerosol plumes and light areas represent clear air or the night time region, as the sun was rising in the east at this time. The red cross represents the aircraft position at 16:10 UTC.
Bottom: Southern California and northern Baja California as depicted by the visible channel of MODIS on the Aqua satellite, at 20:30 UTC, 21 September. The red dots represent active fires.

Title Page

Abstract | Introduction

Conclusions | References

Tables | Figures

|◄ | ►|

◄ | ►

Back | Close

Full Screen / Esc

Printer-friendly Version

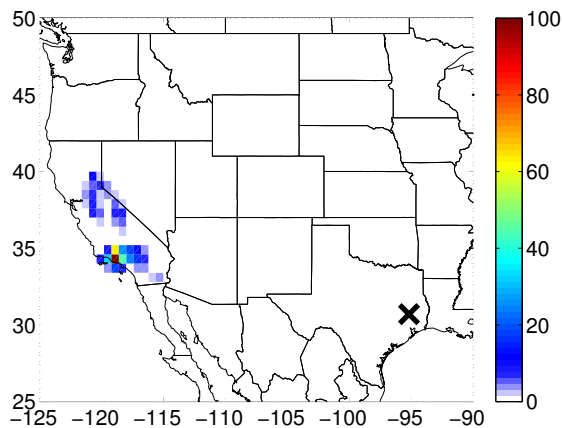Interactive Discussion

EGU

EGU

Fig. 4. Percentage of CO surface contribution of the CO peak measured at about 16:10 UTC due to biomass burning in the main domain output, scaled according to the maximum contribution encountered in the domain output (red pixel).

Printer-friendly Version
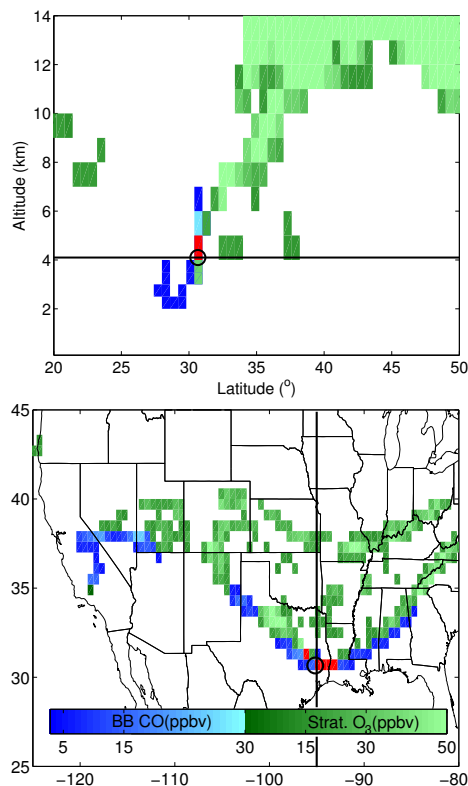
Interactive Discussion

EGU

Fig. 5. (Top) Vertical and (Bottom) horizontal cross sections of the FLEXPART stratospheric ozone tracer (green) and the biomass burning tracer (blue) at 16:00 UTC, 25 September. Grid cells containing both tracers are shaded red. The black circles indicate the aircraft position at 16:10 UTC and the black lines indicate the altitude of the horizontal cross section (top) and the longitude of the meridional cross section (bottom).